

Article

Preliminary Investigation of the Antibacterial Activity of Antitumor Drug 3-Amino-1,2,4-Benzotriazine-1,4-Dioxide (Tirapazamine) and its Derivatives

Evelina Polmickaitė-Smirnova¹, Jonas Šarlauskas^{1,*} , Kastis Krikštopaitis¹, Živilė Lukšienė² , Zita Staniulytė¹ and Žilvinas Anusevičius^{1,*}

¹ Institute of Biochemistry, Life Science Center, Vilnius University, Saulėtekio av. 7, LT-10257 Vilnius, Lithuania; evelina101@gmail.com (E.P.-S.); kastis.krikstopaitis@bchi.vu.lt (K.K.); zita.staniulyte@bchi.vu.lt (Z.S.)

² Institute of Photonics and Nanotechnology, Vilnius University, Saulėtekio av. 10, LT-10223 Vilnius, Lithuania; zivile.luksiene@tmi.vu.lt

* Correspondence: jonas.sarlauskas@bchi.vu.lt (J.Š.); zilvinas.anusevicius@bchi.vu.lt (Ž.A.); Tel.: +370-681-15058 (J.Š.); +370-620-1935 (Ž.A.)

Received: 16 April 2020; Accepted: 8 June 2020; Published: 12 June 2020



Abstract: The antitumor drug 3-amino-1,2,4-benzotriazine-1,4-dioxide (tirapazamine, TPZ (**1**)) along with a number of newly synthesized tirapazamine derivatives (TPZs) bearing substitutions at the 3-amine position of TPZ (**1**) were estimated for their antibacterial activity against representative Gram-negative *Escherichia coli* (ATCC 25922) and *Salmonella enterica* (SL 5676), as well as Gram-positive *Staphylococcus aureus* (ATCC 25923) bacterial strains. Their activities in terms of minimum inhibitory concentrations (MICs) varied in the range of 1.1 μM (0.25 $\mu\text{g/mL}$)–413 μM (128 $\mu\text{g/mL}$). Amongst the most potent derivatives (**1**–**6**), acetyl- and methoxycarbonyl-substituted TPZs (**2** and **4**) were the strongest agents, which exhibited approximately 4–30 fold greater activities compared to those of TPZ (**1**) along with the reference drugs chloramphenicol (CAM) and nitrofurantoin (NFT). The inhibitory activities of the compounds were highly impacted by their structural features. No reliable relationships were established between activities and the electron-accepting potencies of the whole set of studied compounds, while the activities of TPZ drug (**1**) and the structurally uniform set of molecules (**2**–**6**) were found to increase with an increase in their electron-accepting potencies obtained by means of density functional theory (DFT) computation. A greater steric, lipophilic and polar nature of the substituents led to a lower activity of the compounds. The combined antibacterial *in vitro* trial gave clear evidence that TPZs coupled with the commonly utilized antibiotics ciprofloxacin (Cipro) and nitrofurantoin (NFT) could generate enhanced (suggestive of partial and virtually complete synergistic) and additive effects. The strongest effects were defined for TPZs–NFT combinations, which resulted in a notable reduction in the MICs of di-*N*-oxides. These preliminary findings suggest that the synthesized novel di-*N*-oxides might be used as sole agents or applied as antibiotic complements.

Keywords: heterocyclic di-*N*-oxides; 1,2,4-benzotriazine di-*N*-oxides; tirapazamine (TPZ); antibacterial activity; minimum inhibitory concentrations (MICs); chloramphenicol; ciprofloxacin; nitrofurantoin; QSAR; drug combination cooperative behavior

1. Introduction

The discovery of antibiotics raised hope that a powerful tool to control harmful and pathogenic microorganisms has been found. Unfortunately, extensive research has revealed that the fight against microbes remains a constant challenge. For this reason, the development of new drugs with enhanced

antibacterial potencies is still needed ([1–3], and refs. therein). Amid the most plausible, fast and cost-efficient approaches, drugs developed for the treatment of other diseases are also increasingly utilized. Hence, in this context, the testing of drugs used for cancer therapy is becoming a common issue ([2–5], and refs. therein). Cancer and bacterial cells have many properties in common, such as a high replication rate, virulence, ways of spreading within the host, rapid development of resistance mechanisms and a tendency to become more aggressive during disease progression, which implies that some anticancer drugs may act as efficient antibacterial agents, and *vice versa* [2,6–8].

Heterocyclic di-*N*-oxides (HNOXs) have garnered special attention due to their antitumor as well as antiviral and antimicrobial activities ([9–14], and refs. therein). Among them, quinoxaline (benzopyrazine or benzodiazine) di-*N*-oxides (QDNOXs) such as carbadox, olaquinox, mequinox, cyadox, quinocetone etc. were found to be efficient agents against many Gram-positive and -negative bacterial strains ([12–16], and refs. therein). The *N*-oxide moiety of HNOXs with the highest local electrophilic potency is considered to be a key functional (electron-accepting) group governing the redox conversion of these compounds. In this case, the enzymatic (or non-enzymatic) reduction of HNOXs to their free radical intermediates is rapidly accompanied by the generation of reactive oxygen species (ROS) ([12,13], and refs. therein). Recently performed transcriptomic and proteomic studies of *E. coli* strains have provided clear evidence that HNOXs induce ROS generation accompanied by DNA cleavage, involving a substantial contribution of putative reductases in bacteria [12,13]. In general, ROS generation involves a multi-targeting damaging process, in contrast to that of the most antibiotics, which act specifically to a definite target.

Amongst the HNOXs, 3-amino-1,2,4-benzotriazine-1,4-dioxide (tirapazamine (TPZ), SR4233 or WIN 59075) is one of the most prominent anticancer drugs, which underwent phase 2–3 clinical trials and subsequent studies involving liver chemo-embolization. Greater pre-clinical and clinical treatment outcomes were achieved when TPZ was used in combination with other chemotherapeutic agents ([4,17,18], and refs. therein).

TPZ has been shown to be an excellent electron-accepting substrate of extracellular reductases (e.g., NAD(P)H-dependent flavoenzymes such as cytochrome P-450 reductase (P-450R), ubiquinone reductase (complex I), nitric oxide synthase (NOS), etc.), reducing a pro-drug to its radical intermediate, accompanied by ROS generation causing DNA damage, chromosome aberration and other events ([13,19–22], and refs. therein).

In addition to its antitumor activity, tirapazamine has been found to be an efficient antifungal and antibacterial agent with respect to Gram-negative and -positive bacterial strains such as *Escherichia coli* and *Staphylococcus aureus*, respectively, as well as various *Clostridium difficile* strains [4]; antibiotic resistant *E. coli* and *S. aureus* showed virtually the same susceptibility to this drug as wild type strains. Further studies revealed that *E. coli* mutants carrying deletions of genes involved in DNA repair were highly susceptible to TPZ, while those with deleted genes encoding putative reductases showed resistance to TPZ, which suggested that the inhibitory potency of this drug is likely to be caused by its reductive activation by bacterial reductases [4].

Since TPZ functions primarily as a hypoxia selective cytotoxin ([4,11,13,18,22], and refs. therein), it could be predicted to be an efficient agent with respect to bacterial biofilms resembling solid tumors in their heterogeneity of microenvironments, cellular states and anaerobic conditions.

Inspired by the results obtained with heterocyclic di-*N*-oxides (including TPZ) as promising antibacterial agents, in the current work, we estimated TPZ along with a number of newly synthesized derivatives (TPZs) bearing diverse substitutions at the 3-amine position of TPZ (the chemical structures are given in Figure 1) for their inhibitory activities with respect to Gram-negative *Escherichia coli* (*E. coli*, ATCC 25922) and *Salmonella enterica* (*S. enterica*, SL 5676) and Gram-positive *Staphylococcus aureus* (*S. aureus*, ATCC 25923) bacterial strains. These agents have been subjected to quantitative structure-activity relationship (QSAR) analysis using quantum mechanically calculated electron-accepting potency and other molecular descriptors of the compounds. In an effort to render some preliminary evidence for possible therapeutic applications, TPZs were probed in combinations

with broadly utilized conventional antibiotics which revealed enhanced (suggestive of partial or close to complete synergistic) and additive effects.

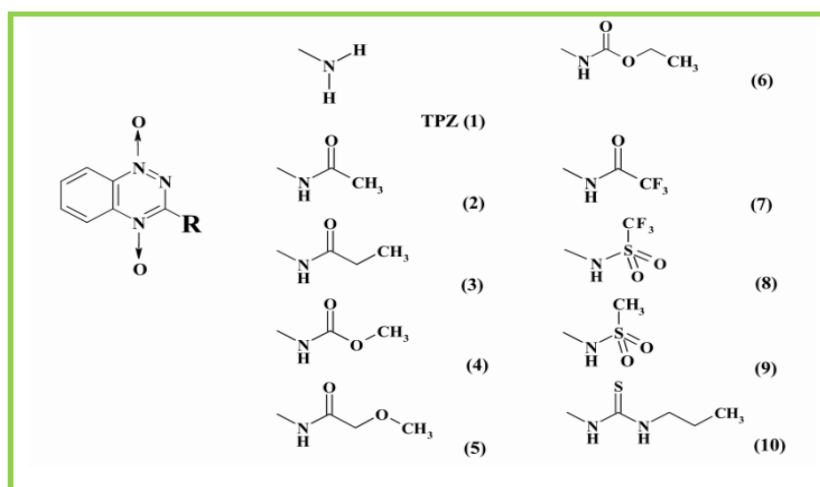


Figure 1. The formulae of 3-amino-1,2,4-benzotriazine-1,4-dioxide (tirapazamine (TPZ (1), SR4233) and its derivatives used in the current work.

2. Materials and Methods

2.1. Reagents and Instrumentation

All chemical reagents and solvents were purchased from commercial suppliers (Sigma-Aldrich, St. Louis, MO, USA), TCI-Europe (Zwijdrecht, Belgium) and Merck (Darmstadt, Germany) and were used without purification unless otherwise specified. Deuterated solvents (d -chloroform or d_6 -dimethylsulfoxide) were obtained from Carl Roth GmbH, Karlsruhe, Germany.

The purity of the compounds was monitored by thin layer chromatography (TLC), using silica gel 60 F254 aluminum plates (Merck, Darmstadt, Germany). The visualization was accomplished by UV light. Flash column chromatography was performed using silica gel Wakogel C-200 (Wako Chemical, Osaka, Japan). The melting points of the compounds were determined in open capillaries by using a MEL-TEMP apparatus (Barnstead Thermolyne Corp., Dubuque, IA, USA). NMR spectra were recorded with a Bruker spectrometer (^1H —400 MHz and ^{13}C —100 MHz) in d -chloroform or d_6 -dimethylsulfoxide by using residual solvent signal as an internal standard. HRMS spectra were recorded by a Dual-ESI Q-TOF 6520 mass spectrometer (Agilent Technologies, Wood Dale, IL, USA) at an interface temperature of 350 °C, a desolvation line (DL) temperature of 250 °C, an interface voltage of ± 4.500 V and neutral DL/Qarray.

2.2. General Procedures for Synthesis of TPZs

3-Amino-1,2,4-benzotriazine 1,4-dioxide (TPZ (1)). The starting 3-amino-1,2,4-benzotriazine 1-oxide was synthesized by the condensation of 2-nitroaniline (2.07 g, 15 mmol) with cyanamide (2.5 g, 15 mmol) suspended in a $\text{CF}_3\text{COOH}/\text{CH}_3\text{COOH}$ mixture (1:1, 50 mL) and heated to 50 °C. Hydrogen peroxide (50 mL, 35% conc.) was introduced, stirred and heated for approximately 12 h, and neutralized by solid KHCO_3 . The final product was filtered, washed with distilled H_2O , dried and purified by flash-column chromatography on silica gel (eluent: ethylacetate). Yield: 78%. ^1H NMR ($\text{CD}_3)_2\text{SO}$) δ 9.83 (bs, 2H, NH_2); 8.43 (d, 2H, $J = 9.6$ Hz); 8.15 (t, 1H, $J = 7.8$ Hz); 7.86 (t, 1H, $J = 7.7$ Hz). HRMS (ESI) m/z [$\text{M}+\text{H}$] $^+$ = 179.0564 (calculated: 179.0563).

3-Acetylamino-1,2,4-benzotriazine 1,4-dioxide (compound 2) was obtained from TPZ (1) (10 mM) dissolved in 10 mL of an acetic acid/acetic anhydride mixture (1:1) heated over a boiling water bath for approximately 10 h. All volatiles were evaporated in vacuo and the remaining solid was re-crystallized from 2-propylacetate. Yield: 76%. Melting point: 201 °C. ^1H NMR (CDCl_3): δ 8.62 (d, 2H, H5 and H8,

J = 4.9 Hz), 8.29 (t, 1H, H6, J = 4.9 Hz) 7.99 (t, 1H, H7, J = 4.9 Hz), 6.52 (bs, 1H, NH), 2.51 (s, 3H, CH₃). HRMS (ESI) m/z [M+H]⁺ = 207.0878 (calculated: 207.0875).

3-Propionylamino-1,2,4-benzotriazine 1,4-dioxide (compound **3**) was synthesized following a similar procedure as described for TPZ (**1**). Yield 48%. Melting point: 167 °C. ¹H NMR (CDCl₃): δ 8.96 (bs, 1H, NH), 8.61 (d, 2H, H5 and H8, J = 4.9 Hz), 8.48 (t, 1H, H6, J = 4.9 Hz), 7.48 (t, 1H, H6, J = 4.9 Hz), 2.80 (q, 2H, CH₂), 1.24 (t, 3H, CH₃); HRMS (ESI) m/z [M+H]⁺ = 235.0829 (calculated: 235.0826).

3-Methoxycarbonylamino-1,2,4-benzotriazine 1,4-dioxide (compound **4**) was obtained following the Schotten–Baumann synthetic procedure by the acylation reaction of TPZ (**1**) (10 mM) in basic medium (10 mL of 10% solution of Cs₂CO₃) with methoxycarbonylchloride (13mM) using aqueous dioxane (50%) as the best reaction medium. The reaction was neutralized by the drop-wise addition of acetic acid. The final product was filtered, washed with distilled H₂O, dried and re-crystallized from acetonitrile. Yield 54%. Melting point: 194 °C. ¹H NMR (CDCl₃): δ 8.92 (bs, 1H, NH), 8.58 (d, 2H, H5 and H8, J = 7.9 Hz), 8.43 (t, 1H, H6, J = 4.7 Hz), 7.44 (t, 1H, H6, J = 4.7 Hz); 0.84 (s, 3H, OCH₃); HRMS (ESI) m/z [M+H]⁺ = 237.0618 (calculated: 237.0617).

Acylated and sulfonylated TPZs (compounds **5**, **7–9**) were obtained following the Schotten–Baumann synthetic procedure by means of the acylation of TPZ (**1**) (10 mM) in basic medium (10% solution of Cs₂CO₃) with carbonylchlorides or sulfochlorides (13 mM) in aqueous dioxane (50%), and the final products were crystallized from ethyl acetate. *3-Methoxyacetyl-amino-1,2,4-benzotriazine 1,4-dioxide* (compound **5**): yield 58%, melting point 170 °C, ¹H NMR (CDCl₃): δ 8.71 (bs, 1H, NH), 8.42 (d, 2H, H5 and H8, J = 9.4 Hz), 8.09 (t, 1H, H6, J = 4.6 Hz), 7.28 (t, 1H, H6, J = 4.6 Hz), 2.31 (s, 2H, CH₂), 0.88 (s, 3H, OCH₃); HRMS (ESI) m/z [M+H]⁺ = 251.0776 (calculated: 251.0774). *3-Ethoxycarbonylamino-1,2,4-benzotriazine 1,4-dioxide* (compound **6**): yield: 62%, melting point: 183 °C, ¹H NMR (CDCl₃): δ 8.66 (bs, 1H, NH), 8.51 (d, 2H, H5 and H8, J = 7.9 Hz), 8.35 (t, 1H, H6, J = 4.7 Hz), 7.18 (t, 1H, H6, J = 4.7 Hz), 2.30 (q, 2H, OCH₂), 1.02 (t, 3H, CH₃). HRMS (ESI) m/z [M+H]⁺ = 251.0772 (calculated: 251.0775). *3-Trifluoroacetyl-amino-1,2,4-benzotriazine 1,4-dioxide* (compound **7**): yield: 52%, melting point: 135 °C, ¹H NMR (CDCl₃): δ 9.22 (bs, 1H, NH), 8.73 (d, 2H, H5 and H8, J = 7.9 Hz), 8.65 (t, 1H, H6, J = 4.7 Hz), 7.39 (t, 1H, H6, J = 4.7 Hz). HRMS (ESI) m/z [M+H]⁺ = 275.0387 (calculated: 275.0384). *3-Trifluoromethyl-sulfonylamino-1,2,4-benzotriazine 1,4-dioxide* (compound **8**): yield: 74%; melting point: 214 °C; ¹H NMR (CDCl₃): δ 9.80 (bs, 1H, NH), 8.81 (d, 2H, H5 and H8, J = 7.8 Hz), 8.45 (t, 1H, H6, J = 4.9 Hz), 7.69 (t, 1H, H6, J = 4.9 Hz); HRMS (ESI) m/z [M+H]⁺ = 311.0058 (calculated: 311.0056). *3-Methylsulfonylamino-1,2,4-benzotriazine 1,4-dioxide* (compound **9**): yield 62%, melting point 241 °C, ¹H NMR (CDCl₃): δ 9.57 (bs, 1H, NH), 8.63 (d, 2H, H5 and H8, J = 7.8 Hz), 8.29 (t, 1H, H6, J = 4.8 Hz), 7.38 (t, 1H, H6, J = 4.8 Hz); HRMS (ESI) m/z [M+H]⁺ = 257.0340 (calculated: 257.0339).

3-Ethoxycarbonylamino-1,2,4-benzotriazine 1,4-dioxide (compound **6**) was obtained following virtually the same synthetic procedure as described for compound **5**. Yield: 62%. Melting point: 183 °C. ¹H NMR (CDCl₃): δ 8.66 (bs, 1H, NH), 8.51 (d, 2H, H5 and H8, J = 7.9 Hz), 8.35 (t, 1H, H6, J = 4.7 Hz), 7.18 (t, 1H, H6, J = 4.7 Hz), 2.30 (q, 2H, OCH₂), 1.02 (t, 3H, CH₃). HRMS (ESI) m/z [M+H]⁺ = 251.0772 (calculated: 251.0775).

3-n-Propylthiocarbamoylamino-1,2,4-benzotriazine 1,4-dioxide (compound **10**) was synthesized by prolonged heating of a mixture of TPZ (**1**) with 1.2 molar equivalents of 1-propylisothiocyanate in dioxane medium at 100 °C for approximately 12 h. All volatiles were removed in vacuo and the resultant product was crystallized from the methylacetate and 2-propanol mixture (1:2). Yield: 43%. Melting point: 292 °C. ¹H NMR ((CD₃)₂SO) δ 9.23 (br.s., 2H, NH-CS-NH); 7.47–8.43 (m, 4H, arom); 3.55 (t, 2H, CH₃CH₂CH₂, J = 6.8 Hz); 1.57 (m, 2H, CH₃CH₂CH₂), 0.90 (t, 3H, CH₃, J = 7.6 Hz). HRMS (ESI) m/z [M+H]⁺ = 280.0861 (calculated: 280.0863).

2.3. Computational Details of TPZs

All quantum mechanical computations of TPZs were performed using the Spartan 10' (Wavefunction Inc., version 1.1.0, 2011, Irvine, CA, USA) software package. To define more stable conformers (compounds **2–10**), a systematic conformational search was conducted by the Merck Molecular Force Field (MMFF)

method by applying the conformational distribution module implemented into Spartan 10' package. The most stable conformers were subjected to further geometric optimization by the restricted Hartree–Fock method (RHF) with a 6–31 G(d,p) basis set. The final optimization and computation of the compounds were carried out by the restricted DFT-B3LYP method coupled with a 6-311+G(d,p) basis set. At each calculation stage, the structures of the compounds were globally optimized without symmetry restrictions and their stationary points were confirmed by frequency analysis. For all the optimized structures, no imaginary frequencies were defined.

For the most stable conformers, conceptual DFT-based global reactivity indices such as the electronic chemical potential (μ) or electronegativity ($\chi = -\mu$), the electronic hardness (η) or softness ($S = 1/\eta$) and the electrophilicity index ($\omega = \mu^2/(2\eta) = (\chi^2/2)S$) were defined using the single-point approach (i.e., at the ground state of neutral molecules) in terms of the lowest unoccupied molecular orbital (LUMO) and the highest occupied molecular orbital (HOMO) energy values, as a crude approximation for the vertical electron affinity ($VEA \approx -E_{LUMO}$) and the vertical ionization potential ($VIP \approx -E_{HOMO}$): $\chi = -(E_{LUMO} + E_{HOMO})/2$ and $\eta = 1/S = E_{LUMO} - E_{HOMO}$ [23–27].

The logarithm of the octanol–water partition coefficient of the compounds ($\log P_{o/w}$) was assessed as the average of the five determinations calculated by applying ACD/Labs (ACD ChemSketch, version C10E41), ALOGPS 2.1 (Virtual Computation Chemistry Laboratory (VCCLAB)), the additive model implemented in XLOGP3 (version 3.2.2) [28], ALOGP based on Ghose, the Pritchett and Crippen method [27] and using the Villar method at the semi-empirical AM1 level [29].

Regression analysis was performed by using Sigma Plot 2000 (SPSS Inc., version 6.10, Chicago, IL, USA) and Statistica (StatSoft Inc., version 8.0, Tulsa, OK, USA) software packages.

2.4. Bacterial Strains

Escherichia coli (ATCC 25922) and *Staphylococcus aureus* (ATCC 25923) were purchased from the American Type Culture Collection (ATCC, Manassas, VA, USA). *Salmonella enterica* serovar Typhimurium (SL 5676) and *Salmonella enterica* (L664) over-expressing the AcrAB-TolC efflux pump system were kindly provided by L. Pidcock (University of Birmingham, UK). The cultures were maintained at 4 °C in Petri dishes with Luria–Bertani (LB) agar containing 10 g/L peptone, 5 g/L yeast extract, 10 g/L NaCl and 15 g/L agar (Sigma-Aldrich Company; St. Louis, MO, USA), and were passaged once a week. Prior to inoculation onto agar plates, the cultures of bacteria tested were grown in Mueller–Hinton broth (MHB) containing 2 g/L beef extract, 17.5 g/L casein hydrolysate and 1.5 g/L starch (Sigma-Aldrich Company; St. Louis, MO, USA) at 37 °C until the optical density at 600 nm reached the value of 0.4 ± 0.1 , corresponding to approximately 2×10^8 colony forming units (CFU) per mL.

2.5. Antibacterial Tests

The inhibitory potencies of the compounds used in the current work were determined by using the agar dilution method, in accordance with Clinical and Laboratory Standards Institute (CLSI) guidelines [30]. The stock solutions of TPZs were prepared by dissolving them in dimethyl sulfoxide (DMSO) (Sigma-Aldrich Company; St. Louis, MO, USA) whose concentration in agar plates did not exceed 2% (v/v), which did not affect the viability of bacterial strains. For each measurement, MH agar medium (containing MHB and 17.0 g/L agar) was added to the container and two-fold diluted (v/v) compounds were infused, mixed well and poured into a Petri dish. The bacterial strains were grown in MH broth at 37 °C. The cell suspensions were adjusted to 1×10^8 CFU/mL by vortexing (diluted 1:10). The final inoculum for the spot was adjusted to the desired cell density (approximately 1×10^4 CFU per spot). The test compounds supplemented onto MH agar plates were incubated for 16 h at 37 °C, and were visually inspected. The lowest concentration of the test compound which completely inhibited visible bacteria growth is considered to be the minimum inhibitory concentration (MIC, in terms of μM and $\mu\text{g/mL}$). An agar plate without any substance (medium and DMSO) and a sterility plate (medium only) were used as negative controls. The conventional antibiotics chloramphenicol (CAM), ciprofloxacin (Cipro) and nitrofurantoin (NFT) (Sigma-Aldrich Company; St. Louis, MO,

USA) were used as the reference drugs. For each concentration of the compounds and antibiotics, the experiments were performed in triplicate on at least two independent occasions.

2.6. Drug Combination Assay

The combinations of TPZs with conventional antibiotics were conducted at varying concentrations of TPZs (by serial two-fold dilution) in the presence of several fixed sub-inhibitory concentrations of antibiotics. The inhibitory activities were assessed by the same method as described above. The obtained results were expressed in terms of the fractional inhibitory concentration index (FICI): $FICI = FIC_A + FIC_B$, where $FIC_A = (\text{MIC of compound A in combination with B})/(\text{MIC of A used alone})$ and $FIC_B = (\text{MIC of compound B in combination with A})/(\text{MIC of B used alone})$, and interpreted as synergism ($FICI \leq 0.5$), partial synergism ($0.5 \leq FICI \leq 0.75$), additive ($0.75 \leq FICI \leq 1$) and indifferent (non-interactive) effect ($1 < FICI \leq 2$) ([31–33], and refs. therein). For each drug combination, FICI values were defined from three independent experiments. For graphical representations, the isobolograms of the combined action of the compounds (by plotting FIC_A versus FIC_B values for the test TPZs and conventional antibiotics, respectively) were generated using the Sigma Plot 2000 (SPSS Inc., version 6.10, Chicago, IL, USA) software package.

3. Results and Discussion

3.1. Antibacterial Activity and QSAR Studies

Table 1 provides the inhibitory potencies of TPZ (1) and a set of its 3-amino substituted derivatives (compounds 2–10) against a panel of *E. coli*, *S. enterica* and *S. aureus* strains in terms of minimum inhibitory concentrations (MICs), which varied in the range of 1.1 μM (0.25 $\mu\text{g/mL}$)–412.6 μM (128.0 $\mu\text{g/mL}$). Note that the activities of the antibacterial compounds are considered significant when the $\text{MIC} \leq 10 \mu\text{g/mL}$, moderate when the MIC varies in the range of 10–100 $\mu\text{g/mL}$, and insignificant when the $\text{MIC} > 100 \mu\text{g/mL}$ [33,34]. TPZ (1) showed significant activity towards Gram-negative *E. coli* and *S. enterica* strains (with MICs of 44.9 μM (8.0 $\mu\text{g/mL}$)), which was twice as high as that as defined against the Gram-positive *S. aureus* strain ($\text{MIC} = 89.8 \mu\text{M}$ (16.0 $\mu\text{g/mL}$)). Of the whole set of the compounds tested, TPZs (compounds 2–6) exhibited the highest activities towards all the strains (MICs varied in the range of 1.1–32.0 μM (0.25–8.0 $\mu\text{g/mL}$)) (Table 1), being close to or markedly higher than those of tirapazamine (1) along with the reference drugs chloramphenicol (CAM) and nitrofurantoin (NFT) (MICs of 8.4–24.8 μM or 2.0–8.0 $\mu\text{g/mL}$) and were less potent than ciprofloxacin (Cipro) (MICs of 0.04–0.08 μM or 0.02–0.06 $\mu\text{g/mL}$). Among the most potent TPZs (2–6), the compound bearing an acetylamino group (2) showed the strongest activity against *E. coli* and *S. enterica* strains (MICs of 1.1 μM (0.25 $\mu\text{g/mL}$)), and two-fold lower potency against *S. aureus* ($\text{MIC} = 2.2 \mu\text{M}$ (0.5 $\mu\text{g/mL}$)). The compound with a methoxycarbonylamino substituent (4) was the second most active agent against *E. coli* with a MIC of 4.2 μM (1.0 $\mu\text{g/mL}$) and with MICs of 2.1 μM (0.50 $\mu\text{g/mL}$) against *S. enterica* and *S. aureus*. The compound bearing a propionylamino group (3) was the third most active agent (MICs of 8.5 μM (2.0 $\mu\text{g/mL}$)) towards *E. coli* and *S. enterica* strains and a MIC of 4.3 μM (1.0 $\mu\text{g/mL}$) against *S. aureus*, which was followed by the ethoxycarbonylamino-TPZ (6), with MICs of 32.0 μM (8.0 $\mu\text{g/mL}$) against *E. coli* and 16 μM (4.0 $\mu\text{g/mL}$) against *S. enterica* strain, while its potency against *S. aureus* was markedly higher (MIC of 4.0 μM (1.0 $\mu\text{g/mL}$)), close to that of the highly active compound 4. Due to its electron-withdrawing characteristic and attractive stereo-electronic profile, the trifluoromethyl group ($-\text{CF}_3$) is applied as one of the most important substituents in pharmaceutical research ([34], and refs. therein). Nonetheless, the substitution of the methyl group of the most active compound 2 with a $-\text{CF}_3$ group (compound 7) led to markedly lower activity towards *E. coli* and *S. enterica* (MICs of 58.4 μM (16.0 $\mu\text{g/mL}$)) and *S. aureus* (MIC of 116.7 μM (32.0 $\mu\text{g/mL}$)). The substitution of the $-\text{COCF}_3$ in compound 7 with $-\text{SO}_2\text{CF}_3$ (compound 8) resulted in a further decline in activity against *E. coli* and *S. enterica* strains (MICs of 412.6 μM (128.0 $\mu\text{g/mL}$)), while the activity of this compound towards *S. aureus* was four-fold higher, close to that of compounds 9 and 10. The negative contribution of the

-CF₃ group is clearly exemplified by comparing the activity of compound **8** with that of compound **9** against Gram-negative bacterial strains. Overall, as shown in Table 1, di-*N*-oxides showed virtually the same inhibitory potencies with respect to both of the Gram-negative strains, with an exception of compounds **4–6**, which showed two-fold higher activities against *S. enterica*. In addition, the activities of the whole set of TPZs towards the Gram-positive *S. aureus* strain (in terms of log 1/MICs = pMICs) well correlated with those towards both Gram-negative bacterial strains (Pearson's R ~ 0.9).

Table 1. The minimum inhibitory concentration (MIC) and inhibitory activity (in terms of pMIC = $-\log$ MIC (μ M)) of TPZ (**1**), its derived compounds (**2–10**) and the reference antibiotics used against Gram-negative (*E. coli* and *S. enterica*) and Gram-positive (*S. aureus*) bacterial strains.

Compound	<i>E. coli</i> ATCC 25922			<i>S. enterica</i> SL 5676			<i>S. aureus</i> ATCC 25923		
	MIC(μ M)	MIC (μ g/mL)	pMIC	MIC(μ M)	MIC (μ g/mL)	pMIC	MIC(μ M)	MIC (μ g/mL)	pMIC
TPZ (1)	44.9	8.0	-1.65	44.9	8.0	-1.65	89.8	16.0	-1.95
(2)	1.1	0.25	-0.04	1.1	0.25	-0.04	2.2	0.5	-0.34
(3)	8.5	2.0	-0.93	8.5	2.0	-0.93	4.3	1.0	-0.63
(4)	4.2	1.0	-0.62	2.1	0.5	-0.32	2.1	0.5	-0.32
(5)	16.0	4.0	-1.20	8.0	2.0	-0.90	8.0	2.0	-0.90
(6)	32.0	8.0	-1.51	16.0	4.0	-1.20	4.0	1.0	-0.60
(7)	58.4	16.0	-1.77	58.4	16.0	-1.77	116.7	32.0	-2.07
(8)	412.6	128.0	-2.62	412.6	128.0	-2.62	103.2	32.0	-2.01
(9)	249.8	64.0	-2.40	249.8	64.0	-2.40	249.8	64.0	-2.40
(10)	114.6	32.0	-2.06	114.6	32.0	-2.06	114.6	32.0	-2.06
Chloramphenicol	12.4	4.0		12.4	4.0		24.8	8.0	
Ciprofloxacin	0.18	0.06		0.09	0.03		0.04	0.02	
Nitrofurantoin	16.8	4.0		33.6	8.0		8.4	2.0	

As noted above, the structural requirements for the cytotoxic/therapeutic activity of HNOX compounds includes the presence of a *N*-oxide moiety as a key functional group governing their reductive conversion, and the electron-accepting potency of the compounds is recognized to be the major driving force for their reductive activation. The enzymatic reactivity as well as the cytotoxic (antitumor or antimicrobial) activity of HNOX compounds, including quinoxaline/benzotriazine di-*N*-oxides, have been defined to correlate to varying extents with their electron-accepting potencies expressed in terms of the experimentally estimated redox potentials and/or quantum mechanically calculated electrophilic potencies ([10,22,35–42], and refs. therein).

Table 2 provides the electron-accepting potency of TPZs in terms of LUMO energies (E_{LUMO}) along with their cDFT-based global reactivity indices (electronegativity (χ), the chemical hardness (η), and the electrophilicity (ω)) [23–26]. The ω index has been used as a suitable descriptor for the prediction of the single- as well as two-electron (hydride) reduction potentials of the electrophilic/redox-active agents, including quinones, nitroaromatics and HNOX compounds. Note that for the neutral systems, this index has been found to be virtually insensitive to the solvent effects [26,43–46]. As shown in Table 2, the electron-accepting potency of TPZs in terms of their ω values fell within a markedly wider range compared to that of E_{LUMO} (i.e., $\Delta\omega = 0.91$ eV vs. $\Delta E_{\text{LUMO}} = 0.56$ eV). All the derived compounds were assessed to possess a higher electron-accepting potency relative to that of tirapazamine.

For the whole set of tested TPZs, we were not able to define reliable dependences between pMICs and the electrophilic potency of the compounds ($R = 0.3\text{--}0.36$); nonetheless, the activity of TPZ (**1**) together with the most active derivatives bearing relatively high homology in terms of their substituents (compounds **2–6**), showed a clear tendency to increase with an increase in their ω values towards *E. coli* ($\text{pMIC} = -9.20 \pm 2.62 + (2.15 \pm 0.68) \omega$; $R = 0.84$, $F = 9.82$), and to a lesser extent against *S. enterica* ($R = 0.77$, $F = 5.60$) or *S. aureus* ($\text{pMIC} = -8.30 \pm 3.21 + (2.00 \pm 0.84) \omega$; $R = 0.77$, $F = 5.51$).

Virtually the same situation has previously been reported for the activities of the diverse structure quinoxaline di-*N*-oxide compounds against *Mycobacterium tuberculosis* [38–40], in which no apparent

correlations have been observed between electrochemical redox potentials and inhibitory activities of the entire series of the compounds, while certain dependences have been found for a small and structurally uniform set of molecules within a narrow range of their redox potentials. These data show that the electron-accepting potency of the compounds as the driving force for their reductive activation cannot alone justify the observed activity.

Table 2. The molecular descriptors of TPZs: LUMO (E_{LUMO}), HOMO (E_{HOMO}) energies, global electronegativity (χ), global hardness (η), global electrophilicity (ω), molecular weight (MW), molecular volume (MV), octanol/water partition coefficient ($\text{Log } P_{\text{oct}}$), polar surface area (PSA), H-bond donor (HBD) and H-bond acceptor (HBA) counts. The Log P values represent the average of the five determinations as described in the Experimental section.

Compound	E_{LUMO}	E_{HOMO}	χ	η	ω	$\text{log } P_{\text{oct}}$	MW/MV	PSA (\AA^2)	HBD/HBA
	(eV)								
TPZ (1)	−3.05	−5.93	4.49	2.88	3.50	0.75±0.58	178.2/157.2	72.21	1/6
(2)	−3.43	−6.34	4.89	2.91	4.10	0.63 ± 0.60	220.2/200.3	70.33	1/7
(3)	−3.40	−6.31	4.86	2.91	4.05	1.18 ± 0.62	234.2/216.4	69.74	1/7
(4)	−3.29	−6.25	4.77	2.96	3.84	0.83 ± 0.54	236.2/207.3	76.59	1/7
(5)	−3.17	−6.13	4.65	2.96	3.65	0.55 ± 0.31	250.2/225.9	75.69	1/8
(6)	−3.21	−6.18	4.70	2.97	3.71	1.29 ± 0.52	250.1/225.9	77.60	1/8
(7)	−3.63	−6.65	5.14	3.02	4.37	1.51 ± 0.56	274.2/212.3	69.17	1/7
(8)	−3.60	−6.64	5.12	3.04	4.37	2.81 ± 0.83	310.2/225.0	92.63	1/9
(9)	−3.41	−6.64	5.03	3.23	3.91	2.25 ± 0.71	256.2/211.0	94.03	1/9
(10)	−3.51	−6.10	4.81	2.59	4.46	1.89 ± 0.67	279.3/256.9	63.00	2/8

Table 2 provides a set of additional indices of the test compounds, including lipophilicity (octanol/water partition coefficient, $\text{Log } P_{\text{oct}}$), molecular weight (MW) and volume (MV), polar surface area (PSA), H-bond donors (HBDs) and H-bond acceptors (HBAs). All compounds followed Lipinski's rule predictive to good bioavailability ($\text{MW} < 500$, $\text{Log } P < 5$, $\text{HBD} < 5$, and $\text{HBA} < 10$) [47]. For the whole set of tested TPZs, the reliable negative dependences between the inhibitory potencies of the compounds and their $\text{Log } P_{\text{oct}}$ values were observed for *E. coli* ($R = 0.84$; $F = 14.63$) and *S. enterica* ($R = 0.86$; $F = 22.69$), while to a markedly lesser extent for *S. aureus* ($R = 0.68$; $F = 7.11$), suggesting that the more hydrophilic nature of the substituents leads to the higher inhibitory activities of TPZ derivatives. Furthermore, the inhibitory potencies of the compounds towards all the tested strains decreased with an increase in their molecular weight ($R = 0.75$ – 0.86), with the exception of TPZ (1), and showed a slight tendency to decrease with an increase in their polarity, expressed in terms of the polar surface area (PSA) ($R = 0.70$ – 0.74) and the H-bond acceptor counts (HBAs) ($R = 0.55$ – 0.60), by excluding the low potent derivative (10).

3.2. Combinations of TPZs with Conventional Antibiotics

The use of combination therapy is commonly justified by the following reasons: to extend the spectrum of drug action (important for heavy infections where early treatment is critical); to prevent or delay the emergence of drug resistance and achieve enhanced (partial or complete synergistic) or at least additive effects, which should allow for the use of a lower dosage of single agents (thereby reducing the risk of their toxic and other side effects) ([14,31–33,48], and refs. therein). Over the past decades, a good deal of work has been done on the anticancer activity of HNOXs, including tirapazamine (1) and its derivatives in combinations with other antitumor drugs (most notably platinum complexes and alkylating agents) which typically exhibited synergistic or additive effects ([18,49–51], and refs. therein). In contrast, to our knowledge, there is no previous research into the combined antimicrobial actions of di-*N*-oxides coupled with other drugs, with the exception of the combined study carried out by Zhao et al. [14]. This study assessed the activities of quinoxaline di-*N*-oxides, including the representative drugs cyadox, mequindox and quinocetone with a range of conventional antibacterials towards mycobacteria, mycoplasma and fungi, which at best exhibited additive effects

against *Mycobacterium tuberculosis* and *Mycoplasma gallisepticum* in combination with rifampicin and tetracycline, respectively.

To provide some evidence for the possible therapeutic application of TPZs in combination with other drugs, in this work we have conducted preliminary combined antibacterial tests for the inhibitory potencies of tirapazamine (1) along with its most potent derivative (2) in combination with ciprofloxacin (Cipro) and nitrofurantoin (NFT), which have been chosen as two of the most efficient and broadly utilized conventional antibiotics in clinical practice, particularly in the treatment of urinary tract infections ([52–54], and refs. therein). In addition, Cipro and NFT were shown to have potential as anticancer agents ([55,56], and refs. therein). Along with representative bacterial strains, the inhibitory potencies of TPZs have been probed as sole agents and in combination with conventional antibiotics against the *S. enterica* strain over-expressing the AcrAB-TolC efflux pump system (one of the best examined resistance–nodulation–division (RND) efflux systems), which extrudes a broad variety of structurally unrelated compounds, including different classes of antibiotics; the overproduction of the AcrAB-TolC efflux pump system confers multiple resistance in Gram-negative bacterial strains, including *E. coli* and *S. enterica* serovar Typhimurium ([57–59], and refs. therein).

In the current study, Cipro and NFT probed as single agents towards the *S. enterica* strain over-expressing AcrAB-TolC exhibited half as much and four times less activity, respectively, compared to that as defined against *S. enterica* SL 5676 strain (Table 1), while the activities of both the tested TPZs towards the *S. enterica* strain over-expressing AcrAB-TolC were the same as those against *S. enterica* SL 5676, suggesting that in contrast to the standard antibiotics, di-*N*-oxides do not seem to be substrates of the AcrAB-TolC efflux pump system.

As described earlier, TPZ drug (1) along with the lead compound (2) in combination with conventional antibiotics have been quantified for their inhibitory potencies by varying concentrations of the compounds (by sequential two-fold dilution method) in the presence of the fixed sub-inhibitory concentrations of Cipro and NFT. The obtained results are reported in Table 3, along with Figure 2 representing the isobolograms plotted in terms of fractional inhibition concentration (FIC) values of the tested TPZs with Cipro and NFT used alone and in combinations. In Figure 2, the diagonal solid, dashed and dot-dashed lines represent the theoretical lines for additive (FICI ~ 1), partial synergistic ($0.5 \leq \text{FICI} \leq 0.75$) and total synergistic ($\text{FICI} \leq 0.5$) effects, respectively. As can be seen in Table 3 and Figure 2, the combined inhibitory potencies defined with respect to representative Gram-negative and Gram-positive strains fell in the range between weak partial synergistic (or nearly additive) effects (FICI of ~0.75–0.77) and strong partial (or virtually complete) synergistic effects (FICI of ~0.5–0.53).

Table 3. The minimum inhibitory concentration (MIC), the fold potentiation (FP) and the fractional inhibitory concentration index (FICI) of TPZ drug (1) and its most potent derivative (compound 2) in combinations with sub-inhibitory concentrations of conventional antibiotics ciprofloxacin (Cipro) and nitrofurantoin (NFT). The strongest combined effects are indicated in bold.

Combination	<i>E. coli</i> ATCC 25922			<i>S. enterica</i> SL 5676			<i>S. aureus</i> ATCC 25923			<i>S. enterica</i> AcrAB-TolC		
	MIC ($\mu\text{g/mL}$)	FP	FICI	MIC ($\mu\text{g/mL}$)	FP	FICI	MIC ($\mu\text{g/mL}$)	FP	FICI	MIC ($\mu\text{g/mL}$)	FP	FICI
TPZ(1)/Cipro(1/4 MIC)	4.0	2	0.75	4.0	2	0.75	8.0	2	0.75	8.0	1	1.25
TPZ(1)/Cipro(1/2 MIC)	0.5	16	0.56	1.0	8	0.62	2.0	8	0.63	8.0	1	1.50
TPZ (1)/NFT(1/4 MIC)	4.0	2	0.75	4.0	2	0.75	4.0	4	0.50	8.0	1	1.25
TPZ (1)/NFT(1/2 MIC)	0.13	62	0.52	0.03	267	0.50	1.0	16	0.56	8.0	1	1.50
(2)/ Cipro (1/4 MIC)	0.13	2	0.77	0.13	2	0.75	0.25	2	0.75	0.25	1	1.25
(2)/Cipro(1/2 MIC)	0.06	4	0.77	0.06	4	0.75	0.06	8	0.62	0.13	2	1.00
(2) /NFT(1/4 MIC)	0.13	2	0.77	0.13	2	0.77	0.13	4	0.50	0.25	1	1.50
(2) /NFT(1/2 MIC)	0.015	17	0.56	0.0075	36	0.53	0.06	8	0.62	0.13	2	1.00

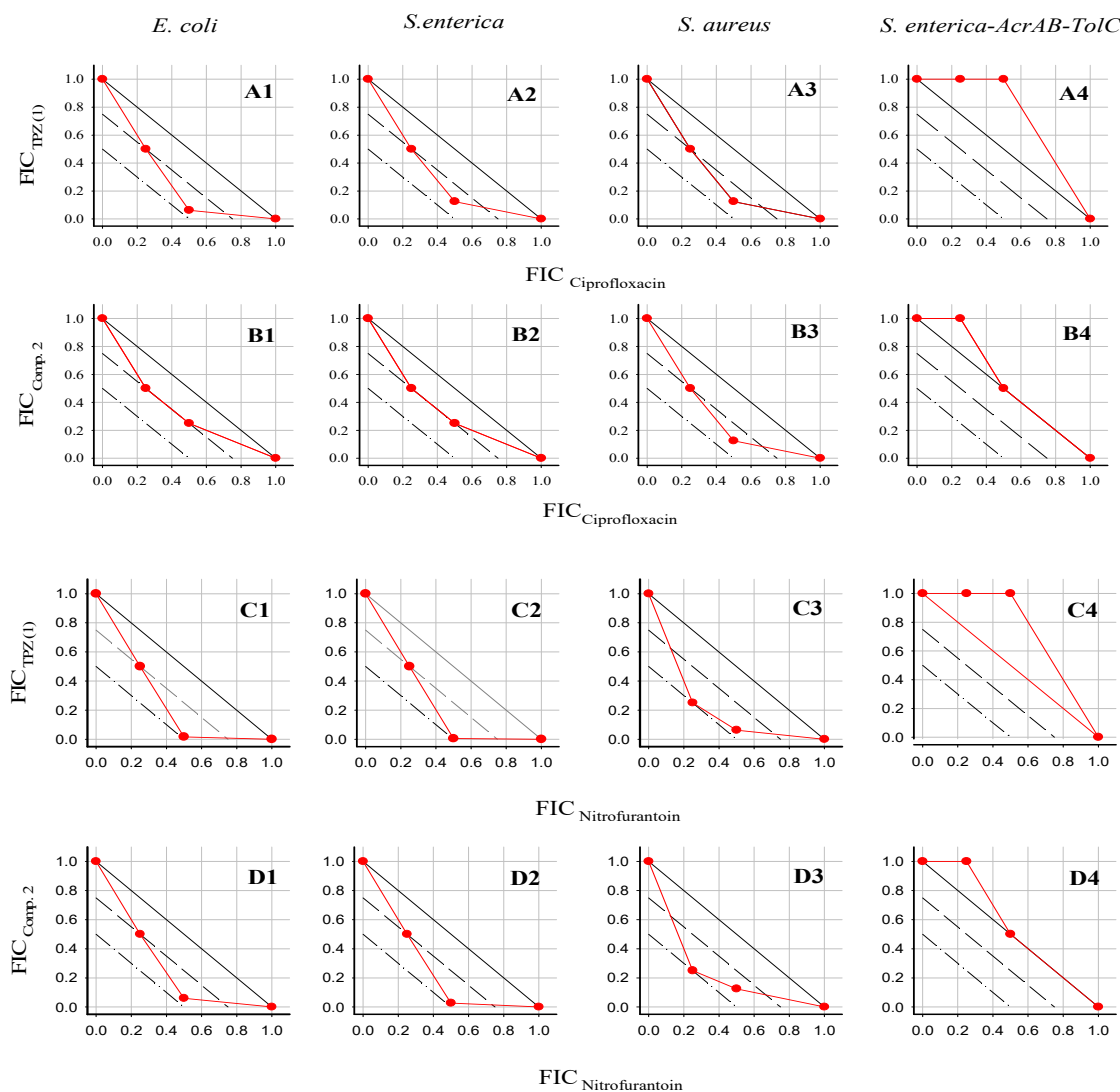


Figure 2. Isobolograms of combinations of TPZ (1) and the lead compound 2 versus ciprofloxacin and nitrofurantoin expressed in terms of their fractional inhibition concentration (FIC) values against Gram-negative *E. coli* (A1–D1) and *S. enterica* (A2–D2) strains, the Gram-positive *S. aureus* strain (A3–D3), and the *S. enterica* strain over-expressing AcrAB-TolC (A4–D4). The straight lines connecting the end points of the y- and x-axis of the FICs of TPZs and antibiotics, respectively, represent total synergistic effect (dot-dashed line), partial synergistic (dashed line) and additive (non-interactive) effect (solid line). All experiments were performed in triplicate on at least two different occasions.

Weak partial synergistic and virtually additive effects (FICI ~0.75–0.77) were defined for the tested compounds by varying their concentrations in the presence of the fixed 1/4 MIC concentrations of Cipro and NFT against the representative Gram-negative and -positive strains, with a two-fold reduction in the MICs of the compounds (note the exception revealed in combinations of TPZs with NFT against the *S. enterica* strain, which resulted in a four-fold reduction in the MICs of di-*N*-oxides (suggestive of complete synergistic effect, FICI ~ 0.5 (Table 3); Figure 2C3,D3).

The markedly greater partial synergistic and virtually complete synergistic effects (with FICI of ~0.56–0.50) were defined for the combined actions of TPZs with the 1/2 MIC concentrations of antibiotics against Gram-negative strains. The strongest combined effects were achieved for the inhibitory potencies of the compounds coupled with the NFT drug, with an approximately 270-fold and 62-fold reduction in the MICs of TPZ (1) against the *S. enterica* strain (FICI ~ 0.50; Figure 2C2) and *E. coli* (FICI = 0.52; Figure 2C1), and followed by a 36- and 17-fold decrease in the MICs of the lead

compound (2) against the *S. enterica* (FICI = 0.53, Figure 2D2) and *E. coli* strain (with FICI of ~0.56; Figure 2D1).

The less pronounced partial synergistic effects were defined for di-*N*-oxides in combination with the 1/2 MIC concentration of Cipro (FICI of 0.56–0.74), with the highest (16-fold) reduction in MIC of tirapazamine (1) against the *E. coli* strain (FICI = 0.56; Figure 2A1) and the lower (eight-fold) reduction in MICs of TPZ (1) against *S. enterica* and *S. aureus* (FICI ~ 0.62–0.63; Figure 2A2,A3), and the same (eight-fold) decrease in MICs of the lead compound (2) against the *S. aureus* strain.

Meanwhile, the same combination assay carried out against the *S. enterica* strain over-expressing AcrAB-TolC revealed only additive and non-interactive effects (FICI of 1.0–1.5) (Table 3); the additive effects have been observed for the lead compound (2) coupled with the 1/2 MIC concentrations of either Cipro or NFT (FICI ~ 1; Figure 2B4,D4).

Overall, the results obtained from the combined *in vitro* trial provided some evidence that di-*N*-oxides coupled with the commonly utilized antibiotics Cipro and NFT could generate enhanced (partial and close to complete synergistic) and additive effects. These findings suggest that TPZs may become valuable antibiotic complements and could be considered as a new choice for the treatment of infectious diseases. The strongest effects were achieved for TPZs coupled with NFT. One of the plausible modes of their action is highly likely to be related to their reductive activation, i.e., single-electron reduction to the free anion radical species accompanied by ROS generation; NFT may undergo a further reduction process through the sequential single- and/or two-electron reduction pathway to its highly reactive nitroso- and/or hydroxylamine intermediate species ([52,53,55], and refs. therein), whilst the anion radical species of TPZs may experience rapid intra-molecular transformation into highly reactive benzotriazinyl radical species ([37], and refs. therein). Hence, on the whole, the production of the reductive intermediates of the compounds along with the amplified ROS generation could be one of the main causes of the multi-factorial antibacterial effects involving multiple cellular targets. Meanwhile, the TPZs coupled with Cipro may exert their inhibitory potencies through at least two major mechanisms, i.e., the inhibition of DNA synthesis by interactions of Cipro with topoisomerase II (DNA gyrase) and topoisomerase IV ([33,54], and refs. therein), along with the reductive activation of TPZs with ROS generation. In addition, one may note that the antibacterial action of Cipro can also induce the production of ROS ([33,60], and refs. therein). A more detailed study needs to be done in order to examine the mode of actions underlying the interactions between the TPZs and antibiotics identified in the current work, which will be one of the subjects of our upcoming research.

4. Conclusions

The anticancer drug tirapazamine (TPZ (1)) has previously been reported to be an efficient antifungal and antibacterial agent [4]. In the present work, TPZ (1) and a series of TPZ analogues, produced by means of a relatively simple, fast and low-cost synthetic procedure, were examined as antibacterial agents towards representative Gram-negative and -positive strains. Amid the most potent compounds (MICs of <10 µg/mL), acetyl- and methoxycarbonyl-substituted TPZs were the strongest agents, exhibiting approximately 4–30 fold greater activities compared to those of TPZ (1), along with the conventional antibiotics chloramphenicol and nitrofurantoin used as reference drugs.

QSAR studies showed that the activities of the tested TPZs were highly impacted by their structural features. The bulky/steric, hydrophobic and polar substituents of the compounds in general led to their lower inhibitory potencies. For TPZ drug (1) along with a virtually uniform set of molecules (2–6), their activities increased with an increase in their electrophilic/electron-accepting potencies, which implies that the activity of the compounds may be partially related to their reductive activation.

TPZ (1) is known to be more active under low oxygen tension ([4,51], and refs. therein). Hence, in the current work, the studies performed for TPZs under aerobic conditions seemingly underestimate their antibacterial effects. It should be noted that antibacterials require a drug safety profile which differs from that of the compounds used as antitumor agents. One should point out that the tolerated dose of TPZ (1) has previously been found to be 390 mg m⁻² ([4], and refs. therein) corresponding to approximately

85 μM (or 15 $\mu\text{g/mL}$), which is twice as high as the dose estimated in the current work against Gram-negative bacteria strains and close to that as defined with respect to the Gram-positive strain. In addition, the combined antibacterial studies performed in the current work gave clear evidence that TPZ compounds coupled with conventional antibiotics can generate additive and synergistic effects, allowing for the use of a lower dosage of the compounds, which could be advantageous as this may decrease the risk of their toxic effects.

Considering TPZs as a source of potential antibacterials, our further research will focus on the synthesis of a broader series of novel di-*N*-oxides based on the structures of the most potent analogues revealed in our work by the introduction of substituents into the benzene ring of the benzotriazine scaffold, along with the estimation of the inhibitory potencies of the compounds used as single agents and in combination with conventional antibiotics. It must be noted, however, that it remains to be proven that TPZs could be safe antibacterial agents. Thus, the assessment of their toxicity and selectivity, as well as the investigation of the mechanistic aspects of their action will also be one of the most important subjects of our forthcoming work.

Author Contributions: Conceptualization, E.P.-S. and Ž.A.; quantum mechanical computation and regression analysis, Ž.A. and K.K.; synthesis and spectral characterization of TPZs, J.Š. and Z.S.; antibacterial study, E.P.-S. and Ž.L.; original draft preparation, Ž.A. All authors have read and agreed to the published version of the manuscript.

Funding: This research was partially supported by the European Social Fund (Measure No. 09.33-LMT-K-712, grant no. DOTSUT-34 (09.3.3-LMT-K712-01-0058/LSS-600000-58).

Acknowledgments: The authors thank Elena Bakienė (Department of Biochemistry and Molecular Biology, Life Sciences Center, Vilnius University) for the technical assistance in microbiological experiments and helpful discussion. The authors also thank Lina Marčiulionytė (Lecturer at Vilnius University) for proofreading the manuscript and highly appreciate the constructive comments and suggestions of the reviewers.

Conflicts of Interest: The authors declare no conflict of interest.

References

1. Fair, R.J.; Tor, Y. Antibiotics and bacterial resistance in the 21st century. *Perspect. Medicin. Chem.* **2014**, *6*, 25–61. [[CrossRef](#)] [[PubMed](#)]
2. Rangel-Vega, A.; Bernstein, L.R.; Mandujano-Tinoco, E.A.; Garcia-Contreras, S.J.; Garcia-Contreras, R. Drug repurposing as an alternative for the treatment of recalcitrant bacterial infections. *Front. Microbiol.* **2015**, *6*, 282. [[CrossRef](#)]
3. Soo, V.W.; Kwan, B.W.; Quezada, H.; Castillo-Juarez, I.; Perez-Eretza, B.; Garcia-Contreras, S.J.; Martinez-Vazquez, M.; Wood, T.K.; Garcia-Contreras, R. Repurposing of anticancer drugs for the treatment of antibacterial infections. *Curr. Top. Med. Chem.* **2017**, *17*, 1157–1176. [[CrossRef](#)] [[PubMed](#)]
4. Shah, Z.; Mahbuba, R.; Turcotte, B. The anticancer drug tirapazamine has antibacterial activity against *E. coli*, *Staphylococcus aureus* and *Clostridium difficile*. *FEMS Microbiol. Lett.* **2013**, *347*, 61–69. [[CrossRef](#)] [[PubMed](#)]
5. Domalaon, R.; Ammeter, D.; Brizuela, M.; Gorityala, B.K.; Zhanel, G.G.; Schweizer, F. Repurposed antimicrobial combination therapy: Tetramycin-ciprofloxacin hybrid augments activity of the anticancer drug mitomycin C against multidrug-resistant Gram-negative bacteria. *Front. Microbiol.* **2019**, *10*, 1556. [[CrossRef](#)] [[PubMed](#)]
6. Waters, C.M.; Bassler, B.L. Quorum sensing: Cell-to-cell communication in bacteria. *Annu. Rev. Cell Dev. Biol.* **2005**, *21*, 319–346. [[CrossRef](#)] [[PubMed](#)]
7. Bhattacharya, B.; Mukherjee, S. Cancer therapy using antibiotics. *J. Cancer Ther.* **2015**, *6*, 849–858. [[CrossRef](#)]
8. Dinno, G.P.; Athanassopoulos, C.M.; Missiri, D.A.; Giannopoulou, P.C.; Vlachogiannis, I.A.; Papadopolous, G.E.; Papaioannou, D.; Kalpaxis, D.L. Chloramphenicol derivatives as antibacterial and anticancer agents: Historic problems and current solutions. *Antibiotics* **2016**, *5*, 20. [[CrossRef](#)]
9. Hu, Y.; Xia, Q.; Shanguan, S.; Liu, X.; Hu, X.; Sheng, R. Synthesis and biological evaluation of 3-aryl-quinoline-2-carbonitrile 1,4-di-*N*-oxide derivatives as hypoxic selective antitumor agents. *Molecules* **2012**, *17*, 9683–9696. [[CrossRef](#)]

10. Chopra, S.; Koolpe, G.A.; Tambo-ong, A.A.; Matsuyama, K.N.; Ryan, K.J.; Tran, T.B.; Doppalapudi, R.S.; Riccio, E.S.; Iyer, L.V.; Green, C.E.; et al. Discovery and optimization of benzotriazine di-N-oxides targeting replicating and non-replicating Mycobacterium tuberculosis. *J. Med. Chem.* **2012**, *55*, 6047–6060. [[CrossRef](#)]
11. Mfuh, A.M.; Larionov, O.L. Heterocyclic N-oxides—An emerging class of therapeutic agents. *Curr. Med. Chem.* **2015**, *22*, 2819–2857. [[CrossRef](#)] [[PubMed](#)]
12. Cheng, G.; Li, B.; Wang, C.; Zhang, H.; Liang, G.; Weng, Z.; Hao, H.; Wang, X.; Liu, Z.; Dai, M.; et al. Systematic and molecular basis of the antibacterial action of quinoxaline 1,4-di-N-oxides against *Escherichia coli*. *PLoS ONE* **2015**, *10*, e0136450.
13. Cheng, G.; Sa, W.; Cao, C.; Guo, L.; Hao, H.; Liu, Z.; Wang, X.; Yuan, Z. Quinoxaline 1,4-di-N-oxides: Biological activities and mechanisms of actions. *Front. Pharmacol.* **2016**, *7*, 64–83. [[CrossRef](#)]
14. Zhao, Y.; Cheng, G.; Hao, H.; Pan, Y.; Liu, Z.; Dai, M.; Yan, Z. In vitro antibacterial activities of animal-used quinoxaline 1,4-di-N-oxides against mycobacteria, mycoplasma and fungi. *BMC Vet. Res.* **2016**, *12*, 186–198. [[CrossRef](#)] [[PubMed](#)]
15. Vieira, M.; Pinheiro, C.; Fernandes, R.; Noronha, J.P.; Prudencio, C. Antimicrobial activity of quinoxaline 1,4-dioxide with 2- and 3-substituted derivatives. *Microbiol. Res.* **2014**, *169*, 287–293. [[CrossRef](#)] [[PubMed](#)]
16. Xu, F.; Cheng, G.; Hao, H.; Wang, Y.; Wang, X.; Chen, D.; Peng, D.; Liu, Z.; Yuan, Z.; Dai, M. Mechanisms of antibacterials action of quinoxaline 1,4-di-N-oxides against *Clostridium perfringens* and *Brachyspirahydysenteriae*. *Front. Microbiol.* **2016**, *7*, 1948. [[CrossRef](#)] [[PubMed](#)]
17. Reddy, S.B.; Williamson, S.K. Tirapazamine: A novel agent targeting tumor cells. *Expert. Opin. Investig. Drugs* **2009**, *18*, 77–87. [[CrossRef](#)]
18. Phillips, R. Targeting hypoxia fraction of tumours using hypoxia-activated prodrugs. *Cancer Chemother. Pharmacol.* **2016**, *77*, 441–457. [[CrossRef](#)]
19. Evans, J.W.; Yudah, K.; Delaoussaye, Y.M.; Brown, J.M. Tirapazamine is metabolized to its DNR-damaging radical by intra-nuclear enzymes. *Cancer Res.* **1998**, *58*, 2098–2101.
20. Garner, A.P.; Paine, M.I.J.; Rodriguez-Crespo, I.; Chinje, E.C.; Ortiz de Montellano, P.; Stratford, I.J.; Tew, T.G.; Wolf, C.R. Nitric oxide synthases catalyze the activation of redox cycling and bioreductive anticancer agents. *Cancer Res.* **1999**, *59*, 1929–1934.
21. Shinde, S.S.; Maroz, A.; Hay, M.P.; Denny, W.A.; Anderson, R.E. Characterization of radicals formed following enzymatic reduction of 3-substituted analogues of the hypoxia-selective cytotoxic 3-amine-1,2,4-benzotriazine 1,4-dioxide (tirapazamine). *J. Am. Chem. Soc.* **2010**, *132*, 2591–2599. [[CrossRef](#)] [[PubMed](#)]
22. Nemeikaitė-Čėnienė, A.; Šarlauskas, J.; Janušienė, V.; Marozienė, A.; Misevičienė, L.; Yantsevich, A.V.; Čėnas, N. Kinetics of flavoenzyme-catalyzed reduction of tirapazamine derivatives: Implications for their prooxidant cytotoxicity. *Int. J. Mol. Sci.* **2019**, *20*, 4602. [[CrossRef](#)] [[PubMed](#)]
23. Parr, R.G.; Szentpaly, L.; Liu, S. Electrophilicity index. *J. Am. Chem. Soc.* **1999**, *121*, 1922–1924. [[CrossRef](#)]
24. Pearson, R.G. Absolute electronegativity and hardness correlated with molecular orbital theory. *Proc. Natl. Acad. Sci. USA* **1986**, *83*, 8440–8441. [[CrossRef](#)] [[PubMed](#)]
25. Geerlings, P.; de Proft, F.; Langenaeker, W. Conceptual density theory. *Chem. Rev.* **2003**, *103*, 1793–1873. [[CrossRef](#)]
26. Campadonico, P.R.; Aizman, A.; Contreras, R. Electrophilicity of quinones and its relationship with affinity. *Chem. Phys. Lett.* **2009**, *471*, 168–173. [[CrossRef](#)]
27. Ghose, A.K.; Pritchett, A.; Crippen, G.M. Atomic physicochemical parameters for three dimensional structure directed quantitative structure-activity relationships III. Modeling hydrophobic interactions. *J. Comput. Chem.* **1988**, *9*, 80–90. [[CrossRef](#)]
28. Cheng, T.; Zhao, Y.; Li, X.; Lin, F.; Xu, Y.; Zhang, X.; Li, Y.; Wang, R.; Lai, L. Computation of octanol-water partition coefficients by guiding an additive model with knowledge. *J. Chem. Inf. Model.* **2007**, *47*, 2140–2148. [[CrossRef](#)]
29. Richards, N.G.J.; Williams, P.B.; Tute, M.S. Empirical methods for computing molecular partition coefficients II. Inclusion of conformational flexibility within fragment based approaches. *Int. J. Quantum. Chem.* **1992**, *44*, 219–233. [[CrossRef](#)]
30. Clinical and Laboratory Standards Institute. *Methods for Dilution Antimicrobial Susceptibility Tests for Bacteria that Grow Aerobically—Eighth Edition: Approved Standard M08-A8*; CLSI: Wayne, PA, USA, 2009.
31. Bacon, A.E.; McGrath, S.; Fekety, R.; Holloway, W.J. In vitro synergy studies with *Clostridium difficile*. *Antimicrob. Agents Chemother.* **1991**, *35*, 582–583. [[CrossRef](#)]

32. Orhan, G.; Bayram, A.; Zer, Y.; Balci, I. Synergy tests by E test and checkerboard methods of antimicrobial combinations against *Brucellamelitensis*. *J. Clin. Microbiol.* **2005**, *43*, 140–143. [[CrossRef](#)] [[PubMed](#)]
33. Vitorino, G.P.; Becerra, M.C.; Barrera, G.D.; Caira, M.R.; Mazzieri, M.R. Cooperative behavior of flouroquinolone combination against *Escherichia coli* and *Staphylococcus aureus*. *Biol. Pharm. Bull.* **2017**, *40*, 758–764. [[CrossRef](#)] [[PubMed](#)]
34. Druzhinin, S.V.; Balenkova, E.S.; Nenajdenko, V.G. Recent advances in the chemistry of a,b-unsaturated trifluoromethylketones. *Tetrahedron* **2007**, *63*, 7753. [[CrossRef](#)]
35. Crawford, P.W.; Scamehorn, R.G.; Hollstein, U.; Ryan, M.D.; Kovacic, P. Cyclic voltammetry of phenazines and quinoxalines including mono—An di-N-oxides. Relation to structure and antimicrobial activity. *Chem. Biol. Interact.* **1986**, *60*, 67–84. [[CrossRef](#)]
36. Hay, M.P.; Gamage, S.A.; Kovacs, M.S.; Pruijn, F.B.; Anderson, R.F.; Patterson, A.V.; Wilson, W.R.; Brown, J.M.; Denny, W.A. Structure-activity relationships of 1,2,4-benzotriazine N-dioxides as hypoxia selective analogues of tirapazamine. *J. Med. Chem.* **2003**, *46*, 169–182. [[CrossRef](#)]
37. Anderson, R.F.; Shinde, S.S.; Hay, M.P.; Denny, W.A. Potentiation of the cytotoxicity of the anticancer agent tirapazamine by benzotriazine N-oxides: The role of redox equilibria. *J. Am. Chem. Soc.* **2006**, *128*, 245–249. [[CrossRef](#)] [[PubMed](#)]
38. Moreno, E.; Perez-Silanes, S.; Gouravaram, S.; Macharam, A.; Ancizu, S.; Torres, E.; Aldana, I.; Monger, A.; Crawford, P.W. 1,4-di-N-oxide quinoxaline-2-carboxamide: Cyclic voltammetry and relationship between electrochemical behavior, structure and antituberculosis activity. *Electrochem. Acta* **2011**, *56*, 3270–3275. [[CrossRef](#)]
39. Moreno, E.; Ancizu, S.; Perez-Silanes, S.; Torres, E.; Aldana, I.; Monge, A. Synthesis and antimycobacterial activity of new quinoxaline-2-carboxamide 1,4-di-N-oxide derivatives. *Eur. J. Med. Chem.* **2010**, *45*, 4418–4426. [[CrossRef](#)]
40. Moreno, E.; Gabano, E.; Torres, E.; Platts, J.A.; Revera, M.; Aldana, I.; Monge, A.; Perez-Silanes, S. Studies on LogPo/w of quinoxaline di-N-oxides: A comparison of RP-HPLC experimental and predictive approaches. *Molecules* **2011**, *16*, 7893–7908. [[CrossRef](#)]
41. Torres, E.; Moreno-Viguri, E.; Galiano, S.; Devarapally, G.; Crawford, P.W.; Azqueta, A.; Arbillaga, L.; Varela, J.; Birriel, E.; Di Maio, R.; et al. Novel quinoxaline 1,4-di-N-oxide derivatives as new potential antichagasic agents. *Eur. J. Med. Chem.* **2013**, *66*, 324–334. [[CrossRef](#)]
42. Šarlauskas, J.; Nemeikaitė-Čėnienė, A.; Marozienė, A.; Misevičienė, L.; Lesanavičius, M.; Čėnas, N. Enzymatic single-electron reduction and aerobic cytotoxicity of tirapazamine and 1-N-oxide and nor-N-oxide metabolites. *Chemija* **2018**, *29*, 273–280. [[CrossRef](#)]
43. Eschwege, K.G.; Conradie, J. Redox potentials of ligands and complexes- a DFT approach. *S. Afr. J. Chem.* **2011**, *64*, 203–209.
44. About, H.I. Density functional theory calculations of nitrobenzene molecules group. *Br. J. Sci.* **2012**, *6*, 51–60.
45. Beheshti, A.; Norouzi, P.; Ganjali, M.R. A simple and robust method model for predictivity of reduction potential of quinones family: Electronegativity index effect. *Int. J. Electrochem. Sci.* **2012**, *7*, 4811–4821.
46. Šarlauskas, J.; Misevičienė, L.; Marozienė, A.; Karvelis, L.; Stankevičiūtė, J.; Krikštopaitis, K.; Čėnas, N.; Yantsevich, A.; Laurynėnas, A.; Anusevičius, Ž. The study of NADPH-dependent flavoenzyme-catalyzed reduction of benzo[1,2-c]1,2,5-oxadiazole N-oxides (benzofuroxans). *Int. J. Mol. Sci.* **2014**, *15*, 23307–23331. [[CrossRef](#)]
47. Lipinski, C.A. Lead- and drug like compounds; the rule of five revolution. *Drug Discov. Today Technol.* **2004**, *1*, 337–341. [[CrossRef](#)] [[PubMed](#)]
48. Tamma, P.D.; Cosgrove, S.E.; Maragakis, L.L. Combination therapy for treatment of infections with gram-negative bacteria. *Clin. Microbiol. Rev.* **2012**, *25*, 450–470. [[CrossRef](#)] [[PubMed](#)]
49. Jounaidi, Y.; Waxman, D. Combination of bioreductive drug tirapazamine with the chemotherapeutic pro-drug cyclophosphamide for P450/P450-reductase-based cancer gene therapy. *Cancer Res.* **2000**, *60*, 3761–3769.
50. Denny, W.A.; Wilson, W.R. Tirapazamine: A bioreductive anticancer drug to exploit tumor hypoxia. *Exp. Opin. Investig. Drugs* **2000**, *9*, 2889–2901. [[CrossRef](#)]
51. Marcu, L.; Olver, I. Tirapazamine: From bench to clinical trial. *Curr. Clin. Pharmacol.* **2006**, *1*, 71–79. [[CrossRef](#)]
52. Munoz-Davila, M.J. Role of antibiotics in the era of antibiotic resistance. Highlighted nitrofurantoin for the treatment of lowest urinary tract infections. *Antibiotics* **2014**, *1*, 39–40. [[CrossRef](#)] [[PubMed](#)]
53. Olender, D.; Zwawiak, J.; Zaprutko, L. Multidirectional efficacy of biological active nitrocompounds efficacy of biological active nitrocompounds included in medicine. *Pharmaceutic* **2018**, *11*, 54. [[CrossRef](#)] [[PubMed](#)]

54. Sharma, P.C.; Jain, A.; Jain, S.; Pahwa, R.; Yar, M.S. Ciprofloxacin: Review on developments in synthetic, analytical, and medicinal aspects. *J. Enzyme Inhib. Med. Chem.* **2010**, *25*, 577–589. [[CrossRef](#)] [[PubMed](#)]
55. Wang, Y.; Gray, J.P.; Mishin, V.; Heck, D.E.; Lashin, D.L.; Lashin, J.D. Role of cytochrome P-450 reductase in nitrofurantoin-induced redox cycling and cytotoxicity. *Free Radic. Biol. Med.* **2008**, *44*, 1169–1179. [[CrossRef](#)] [[PubMed](#)]
56. Yadav, V.; Talwar, P. Repositioning of fluoroquinolones from antibiotic to anticancer agents: An underestimated truth. *Biomed. Pharmacother.* **2019**, *111*, 934–946. [[CrossRef](#)]
57. Piddock, L.J.V.; White, D.G.; Gensberg, K.; Pumbwe, L.; Griggs, D.J. Evidence for an efflux pump mediating multiple antibiotic resistance in *Salmonella enterica* serovartyphimurium. *Antimicrob. Agents Chemother.* **2000**, *44*, 3118–3121. [[CrossRef](#)]
58. Giraud, E.; Cloeckert, A.; Kerboeuf, D.; Chaslus-Dancla, E. Evidence for active efflux as the primary mechanism of resistance to ciprofloxacin in *Salmonella enterica* Serovar Typhimurium. *Antimicrob. Agents Chemother.* **2000**, *44*, 1223–1228. [[CrossRef](#)]
59. Chen, S.; Cui, S.; McDermott, P.F.; Zhao, S.; White, D.G.; Paulsen, I.; Meng, J. Contribution of target gene mutations and efflux to decreased susceptibility of *Salmonella enterica* serovar typhimurium to fluoroquinolones and other antibacterials. *Antimicrob. Agents Chemother.* **2007**, *51*, 535–542. [[CrossRef](#)]
60. Goswami, M.; Mangoli, S.H.; Jawali, N. Involvement of reactive oxygen species in the action of ciprofloxacin against *Escherichia coli*. *Antimicrob. Agents Chemother.* **2006**, *50*, 949–954. [[CrossRef](#)] [[PubMed](#)]



© 2020 by the authors. Licensee MDPI, Basel, Switzerland. This article is an open access article distributed under the terms and conditions of the Creative Commons Attribution (CC BY) license (<http://creativecommons.org/licenses/by/4.0/>).